Chapter 1

Phase Transformations in Duplex Stainless Steel: An Assessment by In Situ X-Ray Diffraction

Adriana da Cunha Rocha,
Andrea Pedroza da Rocha Santos and
Gabriela Ribeiro Pereira

Additional information is available at the end of the chapter

http://dx.doi.org/10.5772/intechopen.81128

Abstract

Duplex stainless steels (commonly known as DSS) are a class of stainless steels with a microstructure formed by two main phases: ferrite and austenite. They are used in a wide range of applications, such as chemical processing, in maritime environments and in the oil and gas industries. In most cases, DSS are chosen based on their strength and corrosion resistance for various environments. When exposed to temperatures above 600°C though, the balance of alloying elements can be modified due to precipitation of various secondary phases, such as sigma (σ) and chi (χ). The sigma phase is typically enriched with Cr and Mo, so its formation can lead to a drastic deterioration in toughness, corrosion resistance, and weldability of duplex stainless steels. To prevent damages to these steels due to the formation of sigma phase, the understanding of such transformation becomes mandatory, not only during the development of these steels but also during their processing. In this research, samples from a lean duplex steel UNS S32304 are subjected to a temperature of 800°C and analyzed in situ by X-ray diffraction. Thus, the kinetics of phase transformations occurring in duplex stainless steels are observed in real time.

Keywords: duplex stainless steels, sigma phase, X-ray diffraction, in situ measurements, lean duplex steel

1. An introduction to duplex stainless steels

1.1. Historical background

The first-generation duplex stainless steels, produced in the 1930s, had a satisfactory performance and have been used for a variety of process industry applications including vessels, heat exchangers, and pumps but had limitations in the as-welded condition because of its excessive ferrite content. The introduction of new refining processes [such as the argon oxygen decarburization (AOD)] opened the possibility of a broad spectrum of new stainless steels. Also, the addition of nitrogen as an alloying element made it possible to increase toughness and corrosion of the heated affected zone resistance approaching that of the base metal in the as-welded condition.

The second-generation duplex stainless steels were defined by their nitrogen alloying. This new commercial development, which began in the late 1970s, coincided with the development of offshore gas and oil fields in the North Sea and the demand for stainless steels with excellent chloride corrosion resistance, good fabricability, and high strength. Duplex 2205 stainless steel became the workhorse of the second-generation duplex grades and was used extensively for gas gathering line pipe and process applications on offshore platforms. The high strength of these steels allowed for reduced wall thickness and reduced weight on the platforms and provided considerable incentive for their use [1].

Recent developments in stainless steels are driven, among other factors, by the low cost of the final material, which led to the evolution of the duplex stainless steel subgroup known as "lean duplex." The main objective is the development of DSS with lower content of alloying elements than standard duplex stainless steels [2]. They present as typical chemical composition 20–24% of chromium, 1–5% of nickel, 0.1–0.3% of molybdenum, and 0.10–0.22% of nitrogen. Besides that, its mechanical properties are twice as great as that of austenitic steels, and it has better corrosion resistance and higher yield strength allowing a reduction in the thickness of many final products [3].

1.2. Alloying elements and secondary phases

The constant evolution of stainless steels resulted in complex compositions containing significant alloying elements, such as chromium, nitrogen, nickel, and molybdenum. To achieve a stable duplex structure that responds well to processing and fabrication, care must be taken to obtain the correct level of each of these elements, since adding them to the steel will affect its mechanical and corrosion properties [4, 5].

The benefits of adding alloying elements are attached to unavoidable disadvantages, the main one being a microstructural instability of the material. During processing or use, duplex stainless steels are subject to various phase transformations caused by temperature and time variations, leading to precipitation of various secondary phases. The most common are precipitated austenite, nitrides, carbides (mostly $M_{23}C_6$ type), and intermetallic elements phases, such as sigma (σ) and chi (χ). The formation of such phases is undesirable as they

may cause a significant decrease in corrosion resistance and reduction of the mechanical properties of the material. Therefore, careful processing is necessary to avoid or at least to minimize such transformations [6, 7].

The schematic time-temperature-transformation (TTT) diagram from **Figure 1** shows the typical ranges of temperature and time for precipitation of principal phases in duplex stainless steels. It is observed that the precipitation of the principal intermetallic phases occurs in temperatures above 600°C. Care should be specially taken for the formation of sigma phase, because certain amounts of this phase are extremely detrimental for the mechanical and corrosion properties of theses steels. Therefore, previous knowledge of this amount is extremely important in order to assess the steel.

1.3. The sigma phase

Sigma phase is a nonmagnetic intermetallic phase, rich in iron, chromium, and sometimes molybdenum that presents a complex tetragonal crystalline structure [8]. Its presence affects negatively the mechanical properties, corrosion resistance, and weldability of duplex stainless steels. Precipitation of sigma phase occurs in the duplex stainless steels when these are subjected to high temperatures, either by casting, welding, forging, and aging, as reported by many authors [9–11].

Villanueva et al. [12] successfully showed that sigma phase precipitates preferentially on the austenite/ferrite grain boundaries (**Figure 2**), consuming the ferrite-forming elements (iron and chromium) and growing toward this phase. Similar reports were made by Magnabosco [13], where it is observed that sigma phase precipitation is between 600 and 1000°C, the fastest precipitation rate is occurring around 800–850°C. *Sigma* phase can precipitate by three distinct mechanisms: nucleation and growth from the original ferrite, eutectoid transformation of ferrite into secondary austenite and sigma, and growth from austenite after the total consumption of original ferrite. In any case, the 800°C temperature range is the one to be observed [13, 14].

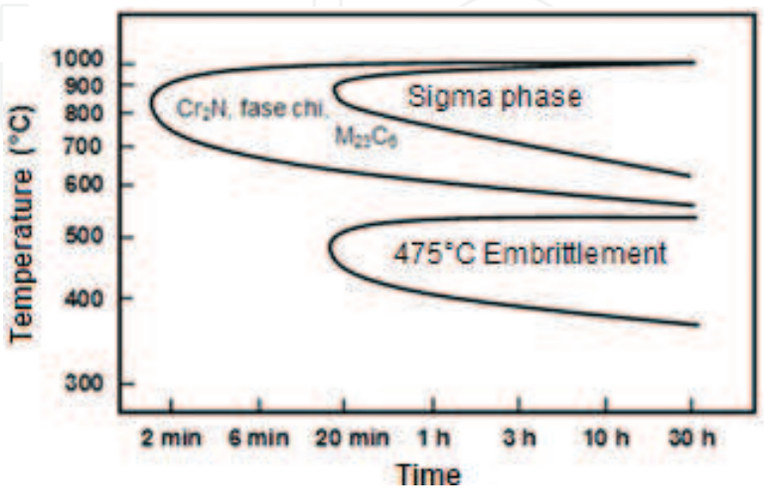

Figure 1. Kinetics of precipitation of different phases in duplex stainless steel [7].

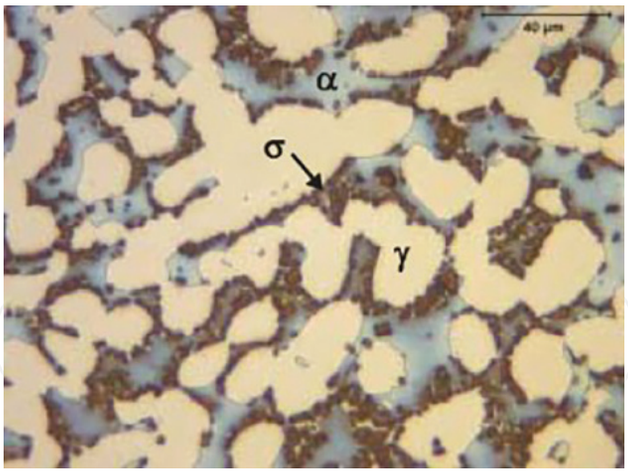

Figure 2. Optical micrograph showing the microstructure of the sample after the heat-treating cycle. Ferrite (α), austenite (γ), and sigma (σ) phase are indicated [10].

2. X-ray diffraction

X-ray diffraction (XRD) is an extremely important analytical technique in the field of microstructural characterization of materials, allowing to obtain information of the order of 10^{-8} cm (1 Å) [15]. Its applications include identification and characterization of crystalline materials, determination of crystal structures, and quantification of phases, both using Rietveld method, textural measurements, residual stress, among others.

Data acquisition to study kinetics at non-ambient conditions is possible with a combination of the XRD equipment with a temperature chamber. X-ray diffraction at non-ambient conditions can be used for a variety of applications, including the study of dynamic processes that need to be investigated in situ, such as phase transformations, oxidation reactions, and crystallite growth.

3. The Rietveld method

The Rietveld method is a mathematical method that performs an adjustment of data on crystalline structures of materials analyzed by X-ray diffraction. In this method, least-square refinements are carried out until the best fit is obtained between the entire observed powder diffraction pattern and the full calculated pattern, as represented in **Figure 3**. The method itself performs the adjustment of data taking into account the total scan and not only one phase of the material [16, 17].

The quantity minimized in the least-square refinement is the residual S_y and is calculated according to Eq. (1):

$$S_y = \sum_i W_i (y_i - y_{ci})^2 \quad (1)$$

where $W_i = 1/y\_i$, y_i = observed intensity at the i-th step, and y_{ci} = calculated intensity at the i-th step.

http://dx.doi.org/10.5772/intechopen.81128

The method's basic premise is that no efforts should be made in advance to allocate observed intensity to particular Bragg reflections or to resolve overlapped reflections. Therefore, it is necessary that a good starting model is used. In this case, different Bragg reflections contributing to a specific intensity y_i are taken into account at every specific i point in the whole pattern. The calculation of intensities can be performed considering the structure factor F_k, for the K_{th} Bragg reflection. This is done by summing the calculated contributions from neighboring Bragg reflections (within a specific range) plus the background, as described in Eq. (2):

$$y_{ci} = s \sum_k L_k F_k^2 \Phi(2\theta_i - 2\theta_k) P_k A + y_{bi} \quad (2)$$

where y_{ci} = calculated intensity of radiation in the i-th step, s = scale factor, k = represents the Miller indices hkl for a Bragg reflection, L_k = contains the Lorentz polarization and multiplication factors, F_k = structure factor modulus for the K_{th} Bragg reflection, Φ = reflection profile function, P_k = preferred orientation function, A = material absorption factor, and y_{bi} = background intensity at the i-th step.

In the quantitative phase analysis using the Rietveld method, the relative weight fraction W of each phase p in a mixture of n phases is calculated according to Eq. (3):

$$W_p = \frac{S_p (ZMV)_p}{\sum_{j=1}^{N} S_j (ZMV)_j} \quad (3)$$

where W_p = weight fraction of phase p, S = Rietveld scale factor, Z = number of formula units per unit cell, M = mass of the formula unit (in atomic mass units), and V = unit cell volume.

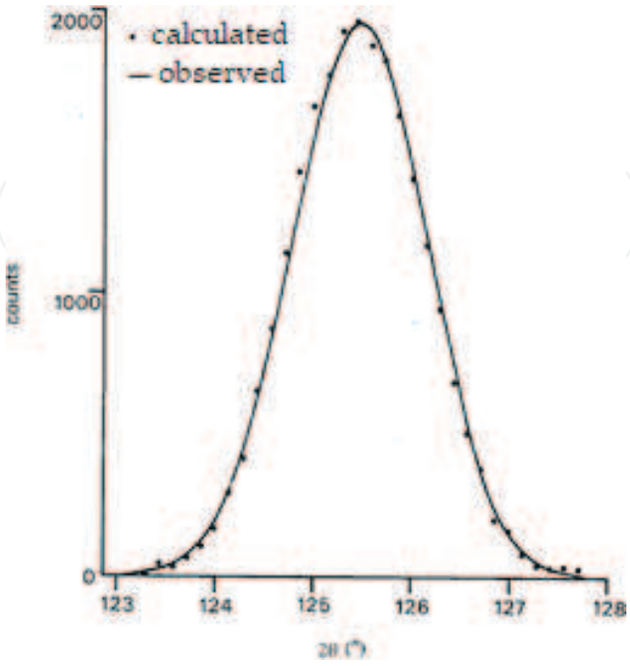

Figure 3. Adjustment by the Rietveld method [17].

4. Experimental procedures

4.1. Chemical composition of steel alloys

Samples with dimensions 20 mm × 20 mm × 1.5 mm were taken from a lean duplex steel plate UNS S32304, with chemical composition presented in **Table 1**.

4.2. In situ high-temperature X-ray diffraction

In situ high-temperature X-ray diffraction data were collected using a *Bruker D8 Discover* diffractometer with a domed hot stage *Anton Paar-DHS 900* (temperature range of 25–900°C), depicted in **Figure 4**. The source of radiation used was cobalt, with a wavelength of 1789 Å.

Diffraction patterns were initially collected at room temperature (30°C). Samples were then heated at 800°C, with an average rate of 1°C/s, and remain at this temperature for 30, 60, or 90 min. At 800°C, the diffraction patterns were collected at every 10 min. At the end of each time interval, cooling was performed at an average rate of 1°C/s till it reaches room temperature.

The main phases were identified by indexing the peaks in the EVA program using the diffraction patterns database provided by PDF Maint. Quantitative phase analysis of the samples was performed using the Rietveld method [16, 17] aided by Topas software.

4.3. OM and SEM-EDS characterization

Metallographic analyses were performed under a *Zeiss* optical microscope (OM), using the AxioVision Rel. 4.7 program, using the light field reflection technique. To obtain a better

C	Co	Cu	Cr	Fe	Mn	Mo	N	Ni	Si
0.036	0.128	0.418	22.670	70.000	1.290	0.117	0.110	4.640	0.385

Table 1. Chemical composition of the lean duplex steel (%wt).

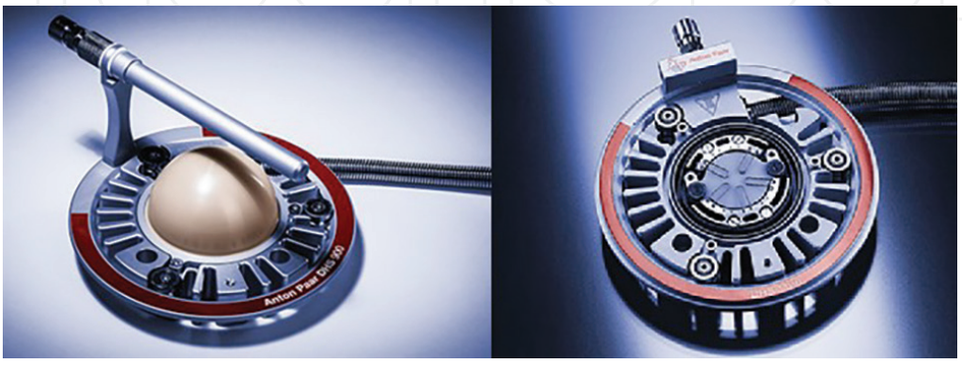

Figure 4. Oven coupled to the X-ray diffractometer.

http://dx.doi.org/10.5772/intechopen.81128

differentiation between ferrite/austenite and the secondary phases formed, an electrolytic attack with 40% NaOH solution was carried out, with 0.2 V for 300 s. Scanning electron microscopy (SEM) with backscattered electrons and EDS analysis was also performed.

5. Results

5.1. Microstructure

Optical microscopy analysis revealed the existence of three distinct regions (white, gray, and brown) in all heated samples, as observed in **Figures 5–7**. The three regions found in the micrographs can be related to presence of the ferrite (δ), austenite (γ), and sigma phase (σ). These observations are in agreement with the results obtained by Jackson et al. [18] for the same selective etching performed in their work, to distinguish these specific phases.

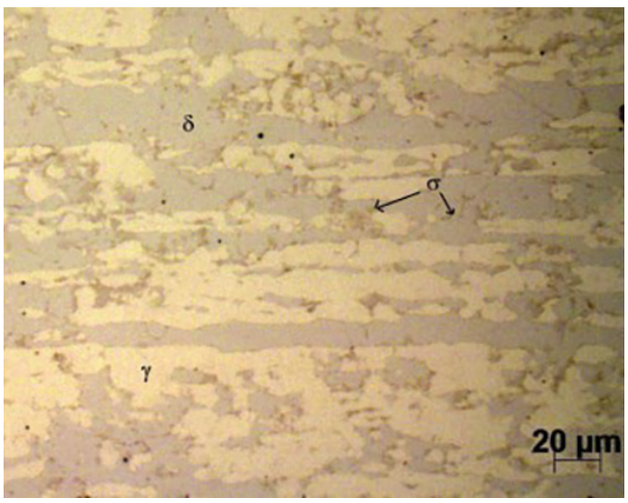

Figure 5. Typical sample after a 30min interval at 800°C.

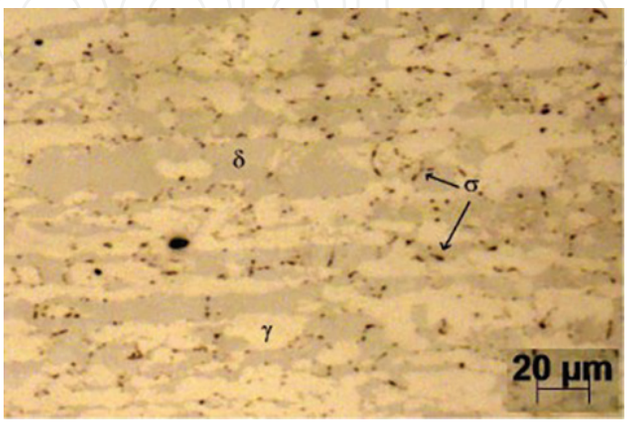

Figure 6. Typical sample after a 60 min interval at 800°C.

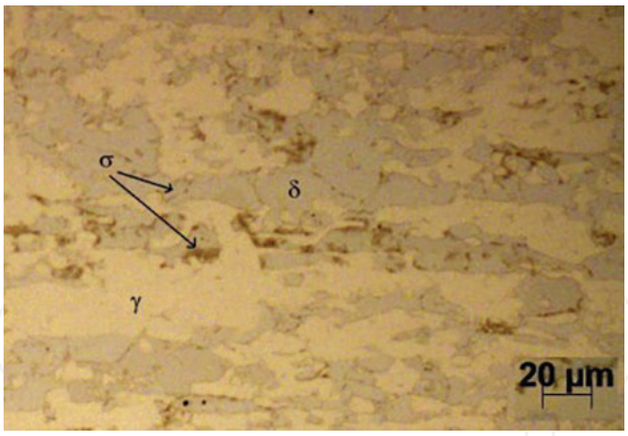

Figure 7. Typical sample after 90 min interval at 800°C.

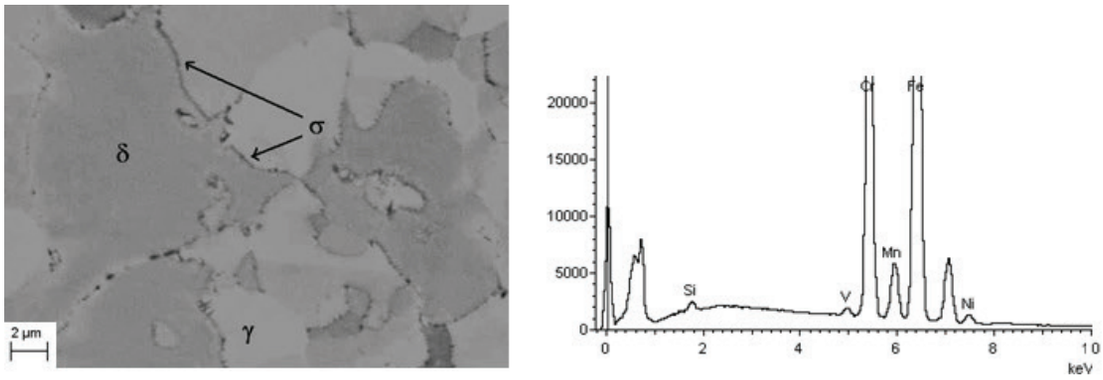

Figure 8. SEM micrographs with the EDS analysis, 30min interval at 800°C.

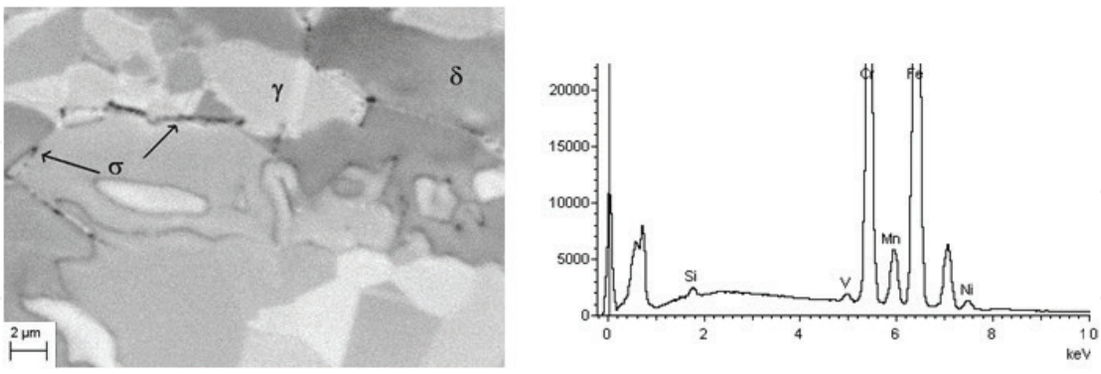

Figure 9. SEM micrographs with the EDS analysis, 60 min interval at 800°C.

Scanning electron microscopy analysis exhibited a similar phase contrast when compared to the optical microscopy results. In this case, three distinct gray areas are observed and related to ferrite (δ), austenite (γ), and sigma phase (σ).

EDS analysis of these same samples observed now by SEM (**Figures 8–10**) exhibits high concentrations of chromium and iron, especially at the grain interfaces, where a darker gray phase is observed. Because sigma phase is mainly formed by Cr and Fe and preferentially has its segregation at the ferrite/ferrite and austenite/ferrite interfaces, one can relate these areas as sigma sites.

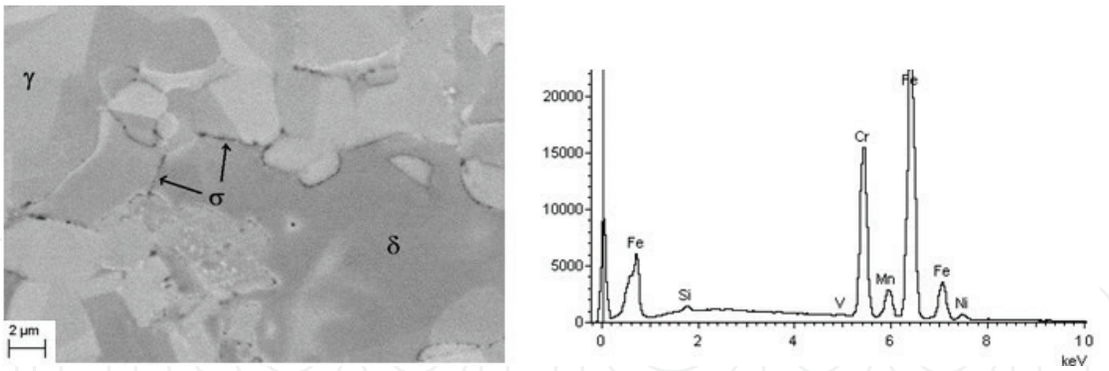

Figure 10. SEM micrographs with the EDS analysis, 90 min interval at 800°C.

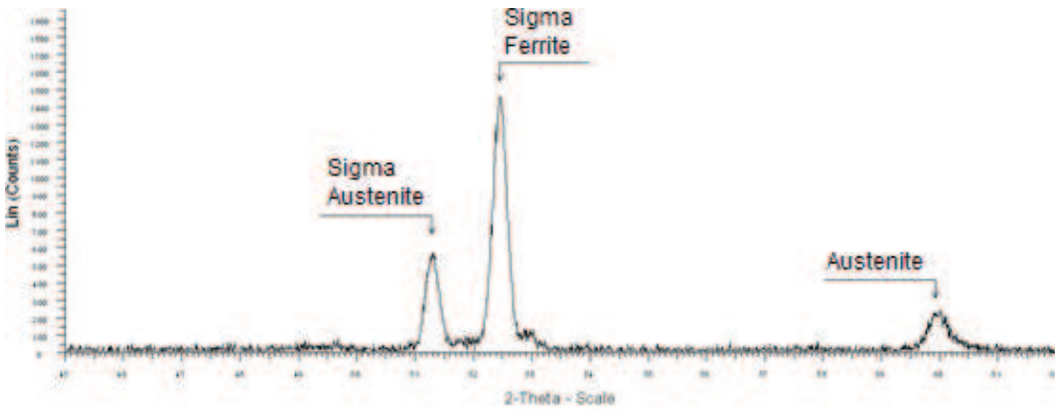

Figure 11. X-ray diffraction pattern at 800°C after 30 min.

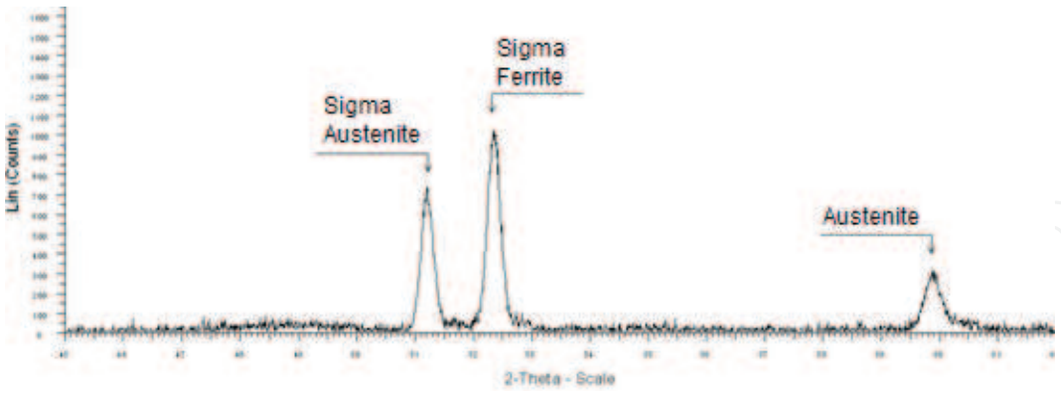

Figure 12. X-ray diffraction pattern at 800°C after 60 min.

5.2. X-ray diffraction patterns

Figures 11–13 show the diffraction patterns of each sample obtained at the end of the dwell time interval (30, 60, and 90 min) at a temperature of 800°C. Through these, it is possible to verify the presence of the ferrite, austenite, and sigma phases.

X-ray diffraction patterns provided the necessary data for the phase quantification in the lean duplex steel. Diffraction was initially performed at room temperature (30°C), followed by

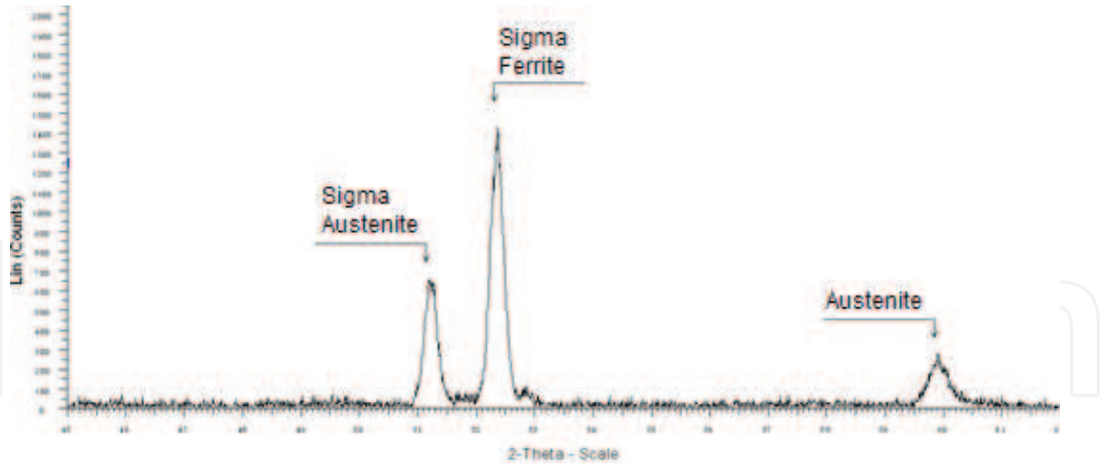

Figure 13. X-ray diffraction pattern at 800°C after 90 min.

Temperature, time	Ferrite	Austenite	Sigma	Ferrite	Austenite	Sigma	Ferrite	Austenite	Sigma
30°C	72.95	27.05	0.00	63.14	36.86	0.00	72.88	27.12	0.00
800°C, 1 min	65.98	32.13	1.89	52.80	44.26	2.94	62.85	36.80	0.35
800°C, 10 min	65.39	31.73	2.88	51.09	42.96	5.95	61.73	37.17	1.10
800°C, 20 min	64.56	32.30	3.14	48.84	43.81	7.35	60.17	37.82	2.01
800°C, 30 min	58.65	29.66	11.49	47.11	43.53	9.36	58.29	38.91	2.80
800°C, 40 min	—	—	—	45.53	43.51	10.96	57.38	39.23	3.39
800°C, 50 min	—	—	—	43.39	43.00	13.61	55.87	38.11	6.03
800°C, 60 min	—	—	—	42.45	41.63	15.92	50.12	34.16	15.72
800°C, 70 min	—	—	—	—	—	—	49.83	34.51	15.67
800°C, 80 min	—	—	—	—	—	—	49.30	34.91	15.79
800°C, 90 min	—	—	—	—	—	—	48.39	34.09	17.52

Table 2. Phase quantification of the lean duplex steel (%vol).

various scans at 800°C at each distinct time interval. **Table 2** presents the values obtained for each phase in the different scan times.

6. The kinetics of phase transformations

In situ X-ray analysis has shown to be effective to determine the kinetics of phase transformation for the evaluation of lean duplex steel phases. **Figures 14–16** present the plotted curves for the transformed amounts of sigma, ferrite, and austenite during the 800°C isothermal heating.

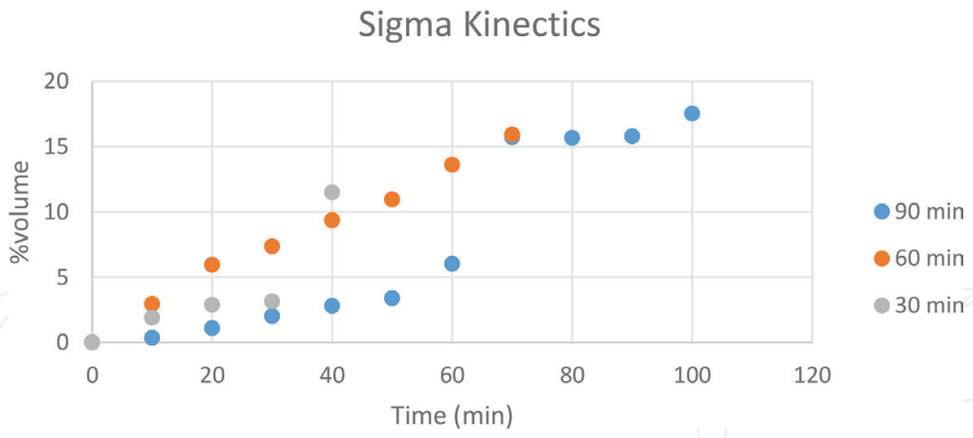

Figure 14. Isothermal evolution of the sigma phase.

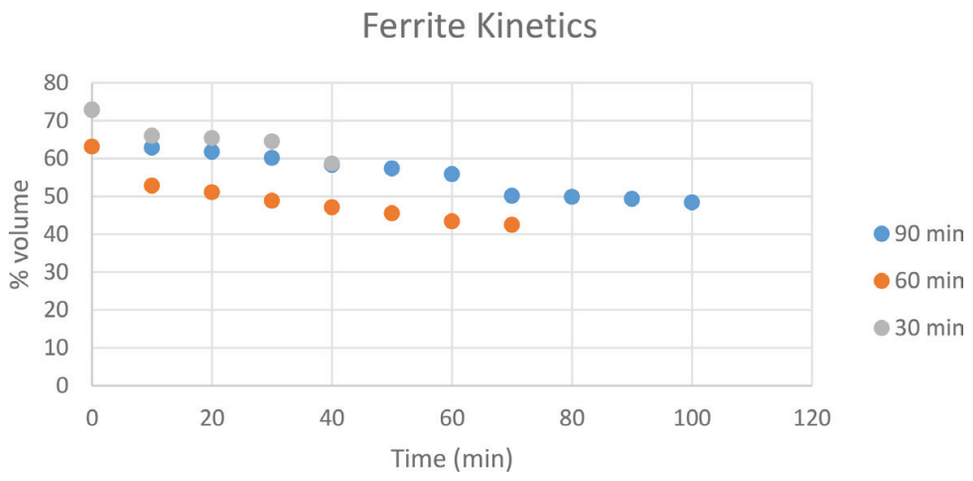

Figure 15. Isothermal evolution of the ferrite phase.

When comparing the evolution of sigma phase (σ) for the 30, 60, and 90 min samples (**Figure 14**), it can be observed that the only one of the three samples that presented a quasi-linear evolution was the 60 min sample, while the two others had a quite variable tendency regarding their volume increase during their isothermal heating. This behavior might be explained by the initial amounts of ferrite and austenite in the 30 and 90 min samples. Both samples had the bigger ferrite/austenite imbalance—that difference in their volume percentage might explain the discontinuities in the speed of sigma formation for those samples, as shown by previous works [13].

Regarding the ferrite evolution, presented in **Figure 15**, it is quite clear that most of its %vol. decrease is related to the sigma formation. Comparing the values for both phases at the same time intervals, it is observed that there is indeed an increase in sigma volume while the ferrite volumes decrease, as reported earlier. That cannot be said from the austenite phase, shown in **Figure 16**. In fact, it is observed that there is a slight increase in austenite volumes along the isothermal heating.

These results lead to the assumption that the sigma formation mechanism is either by continuous or by discontinuous precipitation from ferrite or by a eutectoid decomposition of

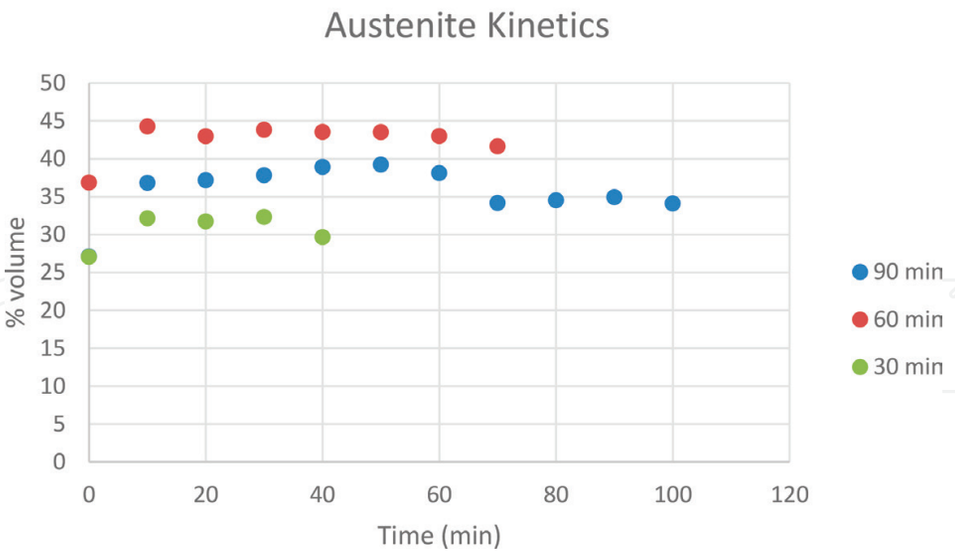

Figure 16. Isothermal evolution of the austenite phase.

ferrite, where a significant decrease in the amounts of ferrite is observed. For this study, it is more likely that the formation of sigma phase is due to the eutectoid decomposition of ferrite because this type of mechanism leads also to the formation of amounts of secondary austenite, therefore increasing its volume over time.

Both mechanisms though lead to Cr- and Mo-depleted phases that will reduce the corrosion resistance of the lean duplex steel, particularly reducing pitting corrosion resistance as reported by earlier works [19, 20]. Wilms et al. [21] also indicated that the formation of sigma has a strong effect on the mechanical properties of stainless steels.

7. Conclusions

Samples of steel UNS S32304 were subjected to isothermal heating at 800°C for 30, 60, and 90 min while analyzed by in situ X-ray diffraction to evaluate the phase transformations occurring at this temperature and time periods. The results lead to the following conclusions:

- Significant amounts of sigma phase were formed during isothermal heating for three time intervals.
- Sigma phase precipitation was observed both in the ferrite/austenite and ferrite/ferrite grain boundaries.
- Depending on the ferrite/austenite balance, sigma phase kinetics may lead to volume percentage of about 15% after 60 min and 17% after a period of 90 min.
- The most likely mechanism for sigma formation on the assessed lean duplex steel is the eutectoid decomposition of ferrite because this type of mechanism leads also to the formation of amounts of secondary austenite, therefore increasing its volume over time.

- Such high percentages of sigma formation lead to Cr- and Mo-depleted phases that will reduce the corrosion resistance of the lean duplex steel, particularly reducing pitting corrosion resistance and jeopardizing the mechanical properties of lean duplex stainless steels.

Acknowledgements

The authors would like to thank CNPq (Brazilian National Council for Scientific and Technological Development) for the support in this research.

Conflict of interest

The authors declare no conflicts of interest.

Author details

Adriana da Cunha Rocha*, Andrea Pedroza da Rocha Santos and Gabriela Ribeiro Pereira

*Address all correspondence to: adrirocha@metalmat.ufrj.br

Department of Metallurgical and Materials Engineering, Federal University of Rio de Janeiro (UFRJ), Rio de Janeiro, RJ, Brazil

References

[1] Davis JR. ASM Specialty Handbook—Stainless Steel. 1st ed. ASM International, Materials Park, Ohio, USA; 1994

[2] Brytan Z, Niagaj J. The lean duplex stainless steel welded joint after isothermal aging heat treatment. Archives of Materials Science and Engineering. 2013;**60**(1):24-31

[3] Souza CS, Lins VFC, Silveira DM. Avaliação da soldagem multipasse de chapas espessas de aços inoxidáveis lean duplex UNS S32304 soldadas pelos processos SMAW, GMAW e FCAW—Parte II: Resistência à corrosão. Soldagem e Inspeção. 2013;**18**(03):257-267

[4] Practical Guidelines for the Fabrication of Duplex Stainless Steels. 2nd ed. Prepared by TMR Stainless. Pittsburgh, PA, USA, London: International Molybdenum Association; 2009

[5] Gunn RN. Duplex Stainless Steels: Microstructures, Properties and Applications. 1st ed. England: Abington Publishing; 1997

[6] Chen TH, Yang JR. Effects of solution treatment and continuous cooling on σ-phase precipitation in a 2205 duplex stainless steel. Materials Science and Engineering A. 2001; **311**(1-2):28-41

[7] Alvarez-Armas I, Degallaix-Moreui S. Duplex Stainless Steels. 1st ed. London: ISTE; 2009

[8] Hall EO, Algie SH. The Sigma Phase. Metallurgical Reviews. 1966;**11**(1):61-88

[9] Calliari I, Brunelli K, Dabala M, et al. Measuring secondary phases in duplex stainless steels. The Journal of the Minerals, Metals & Materials Society. 2009;**61**(1):80-83

[10] Elmer JW, Palmer TA, Specht ED. In situ observations of sigma phase dissolution in 2205 duplex stainless steel using synchrotron X-ray diffraction. Materials Science and Engineering A. 2007;**459**(1-2):151-155

[11] Hsieh C, Wu W. Overview of intermetallic sigma (σ) phase precipitation in stainless steels. ISRN Metallurgy. 2012;**2012**:1-16

[12] Villanueva DME, Junior FCP, Plaut RL, Padilha AF. Comparative study on sigma phase precipitation of three types of stainless steels: Austenitic, superferritic and duplex. Materials Science and Technology. 2006;**22**(9):1098-1104

[13] Magnabosco R. Kinetics of sigma phase formation in a duplex stainless steel. Materials Research. 2009;**12**(3):321-327

[14] Pohl M, Storz O, Glogowski T. Effect of intermetallic precipitations on the properties of duplex stainless steel. Materials Characterization. 2007;**58**(1):65-71

[15] Cullity BD. Elements of X-ray Diffraction. 1st ed. Massachusetts, USA: Addison-Wesley Publishing Company, Reading; 1978

[16] Young RA. The Rietveld Method. 1st ed. New York: Oxford University Press; 1995

[17] Rietveld HM. A profile refinement method for nuclear and magnetic structures. Journal of Applied Crystallography. 1969;**2**(2):65-71

[18] Jackson EMLEM, Visser PE, Cornish LA. Distinguishing between chi and sigma phases in duplex stainless steels using potentiostatic etching. Materials Characterization. 1993;**31**(4):185-190

[19] Fang YL, Liu ZY, Xue WY, et al. Precipitation of secondary phases in lean duplex stainless steel 2101 during isothermal ageing. ISIJ International. 2010;**50**(2):286-293

[20] Magnabosco R, Alonso-Falleiros N. Pit morphology and its relation to microstructure of 850°C aged duplex stainless steel, Corrosion. 2005;**61**:130-136

[21] Wilms ME, Gadgil VJ, Krougman JM, Kolster BH. The effect of σ-phase precipitation at 800°C on the mechanical properties of a high alloyed duplex stainless steel. Materials at High Temperatures. 1991;**9**(3):160-166